

See discussions, stats, and author profiles for this publication at: <https://www.researchgate.net/publication/280388741>

# Chemical Characterization of Urate Hydroperoxide, A Pro-oxidant Intermediate Generated by Urate Oxidation in Inflammatory and Photoinduced Processes

ARTICLE in CHEMICAL RESEARCH IN TOXICOLOGY · JULY 2015

Impact Factor: 3.53 · DOI: 10.1021/acs.chemrestox.5b00132 · Source: PubMed

READS

64

## 10 AUTHORS, INCLUDING:



**Railmara Pereira da Silva**

University of São Paulo

2 PUBLICATIONS 0 CITATIONS

SEE PROFILE



**Paolo Di Mascio**

University of São Paulo

237 PUBLICATIONS 7,277 CITATIONS

SEE PROFILE



**Anthony J Kettle**

University of Otago

134 PUBLICATIONS 6,140 CITATIONS

SEE PROFILE



**Flavia Meotti**

University of São Paulo

39 PUBLICATIONS 1,304 CITATIONS

SEE PROFILE

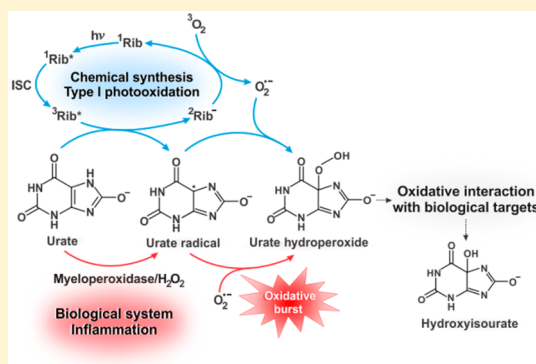
# Chemical Characterization of Urate Hydroperoxide, A Pro-oxidant Intermediate Generated by Urate Oxidation in Inflammatory and Photoinduced Processes

Eliziane S. Patrício,<sup>†</sup> Fernanda M. Prado,<sup>†</sup> Railmara P. da Silva,<sup>†</sup> Larissa A. C. Carvalho,<sup>†</sup> Marcus V. C. Prates,<sup>†</sup> Tony Dadamos,<sup>‡</sup> Mauro Bertotti,<sup>‡</sup> Paolo Di Mascio,<sup>†</sup> Anthony J. Kettle,<sup>§</sup> and Flavia C. Meotti<sup>\*,†</sup>

<sup>†</sup>Departamento de Bioquímica, <sup>‡</sup>Departamento de Química, Instituto de Química (IQUSP), Universidade de São Paulo, 05508-000 São Paulo, SP, Brazil

<sup>§</sup>Centre for Free Radical Research, Department of Pathology, University of Otago, Christchurch, 8140 Christchurch, New Zealand

**ABSTRACT:** Urate hydroperoxide is a strong oxidant generated by the combination of urate free radical and superoxide. The formation of urate hydroperoxide as an intermediate in urate oxidation is potentially responsible for the pro-oxidant effects of urate in inflammatory disorders, protein degradation, and food decomposition. To understand the molecular mechanisms that sustain the harmful effects of urate in inflammatory and oxidative stress related conditions, we report a detailed structural characterization and reactivity of urate hydroperoxide toward biomolecules. Urate hydroperoxide was synthesized by photo-oxidation and by a myeloperoxidase/hydrogen peroxide/superoxide system. Multiple reaction monitoring (MRM) and MS<sup>3</sup> ion fragmentation revealed that urate hydroperoxide from both sources has the same chemical structure. Urate hydroperoxide has a maximum absorption at 308 nm,  $\epsilon_{308\text{nm}} = 6.54 \pm 0.38 \times 10^3 \text{ M}^{-1} \text{ cm}^{-1}$ . This peroxide decays spontaneously with a rate constant of  $k = 2.80 \pm 0.18 \times 10^{-4} \text{ s}^{-1}$  and a half-life of 41 min at 22 °C. Urate hydroperoxide undergoes electrochemical reduction at potential values less negative than  $-0.5 \text{ V}$  (versus Ag/AgCl). When incubated with taurine, histidine, tryptophan, lysine, methionine, cysteine, or glutathione, urate hydroperoxide reacted only with methionine, cysteine, and glutathione. The oxidation of these molecules occurred by a two-electron mechanism, generating the alcohol, hydroxyisourate. No adduct between cysteine or glutathione and urate hydroperoxide was detected. The second-order rate constant for the oxidation of glutathione by urate hydroperoxide was  $13.7 \pm 0.8 \text{ M}^{-1} \text{ s}^{-1}$ . In conclusion, the oxidation of sulfur-containing biomolecules by urate hydroperoxide is likely to be a mechanism by which the pro-oxidant and damaging effects of urate are mediated in inflammatory and photo-oxidizing processes.



## 1. INTRODUCTION

Uric acid (7,9-dihydro-1H-purine-2,6,8(3H)-trione) is the end product of purine nucleotide metabolism in humans. It is a facile electron donor that accumulates in plasma and is, so far, considered to be an important antioxidant for humans.<sup>1,2</sup> The uric acid monoanion, urate ( $\text{pK}_a$  5.4), chelates transition metals ions and reacts with hydroxyl radical, singlet oxygen,<sup>1</sup> and hypochlorous acid.<sup>2–4</sup> In all cases, the main oxidation product detected was allantoin. However, oxonic acid, oxaluric acid, parabanic acid, and cyanuric acid were also identified.<sup>4</sup> Therefore, it seems that, independent of the mechanism, the oxidation of urate generates more soluble and relatively stable products. In agreement with this, one-electron oxidation of urate by peroxidases and hemoproteins also generates allantoin as the main detectable product.<sup>4–6</sup>

Despite the generation of allantoin, a nonharmful end product of urate oxidation, little attention has been focused on the intermediates of urate oxidation. One-electron oxidation of urate by peroxidases generates urate free radical.<sup>7</sup> Urate has

been described as the main electron donor to peroxidases in human plasma.<sup>8</sup> It reacts fast with myeloperoxidase and lactoperoxidase and has been considered to be a physiological substrate for both human enzymes. The urate free radical generated by myeloperoxidase or lactoperoxidase combines with the anion radical superoxide ( $\text{O}_2^{\bullet-}$ ) to yield urate hydroperoxide.<sup>6,9</sup> The fast reaction between urate free radical and superoxide,  $k = 8 \times 10^8 \text{ M}^{-1} \text{ s}^{-1}$ , shows that this is a near-diffusion-limited reaction.<sup>10</sup> These data demonstrate that urate hydroperoxide is a putative intermediate in urate oxidation in vascular inflammatory conditions, where the combination of urate, peroxidases, and superoxide is enhanced.

In agreement with the free radical intermediate mechanism, Clausen and co-workers suggested that urate hydroperoxide is abundantly formed through Type I photo-oxidation, where the triplet light-excited riboflavin transfers one electron from urate

**Received:** March 30, 2015

to oxygen, generating both urate free radical and superoxide.<sup>11</sup> In their experiments, an unstable catalase-resistant hydroperoxide was the main oxidized product, and it appeared to contribute to protein modification and milk decomposition.<sup>11</sup> Urate hydroperoxide is also a putative intermediate in urate oxidase (uricase)-mediated catalysis. However, urate free radical does not seem to be an intermediate in this case.<sup>12,13</sup>

Urate hydroperoxide is a strong oxidizing agent and is different from hydrogen peroxide because it reacts with glutathione in the absence of enzyme catalysis.<sup>6</sup> Therefore, the generation of urate hydroperoxide as an intermediate in urate oxidation is a potentially important mechanism that contributes to the harmful effects of excess urate in either human inflammatory disorders or food decomposition. Determining the precise chemical identity of this hydroperoxide is needed to verify its formation in biological systems. Studying urate oxidation and urate hydroperoxide formation is also required to explore the likelihood that they are involved in alternative oxidative pathways that contribute to redox imbalance in biological systems.

In this study, we report a detailed structural and chemical characterization of urate hydroperoxide generated either by chemical or enzymatic synthesis. The analyses of urate hydroperoxide's redox potential and its reactivity toward biomolecules suggest that urate hydroperoxide may contribute to physiologically relevant oxidative stress.

## 2. MATERIALS AND METHODS

**2.1. Synthesis of Urate Hydroperoxide.** Urate hydroperoxide was synthesized as previously described<sup>11</sup> with minor modifications (see the graphical abstract). A urate (10 mM) stock solution was prepared in 20 mM NaOH, and riboflavin (500  $\mu$ M) was prepared in sodium phosphate buffer (10 mM; pH 6.8). The reaction was carried out in a 340 mm diameter well in a total volume of 4 mL of sodium phosphate buffer (10 mM; pH 6.8), urate (0–600  $\mu$ M), and riboflavin (40  $\mu$ M) under UVA (365 nm) or visible (500 nm; 30 mW) light. The light source was equipped with six UVA lamps, 15 mW, for the UVA source (GE, Novatecnica Campinas-Brasil) or six fluorescent lamps, 30 mW, for the visible light source. The reaction was performed at a controlled temperature of 20 °C with continuous mixing. All solutions were stirred with Chelex (Sigma-Aldrich) for at least 1 h to remove any trace ions.

The synthesis of urate hydroperoxide by myeloperoxidase and superoxide was performed by incubating urate (200  $\mu$ M) with myeloperoxidase (200 nM) in the presence of a superoxide-generating system (0.01 mg/mL xanthine oxidase/10 mM acetaldehyde) in 50 mM phosphate buffer, pH 7.4. The production of superoxide by the xanthine oxidase/acetaldehyde system was monitored by the cytochrome *c* reduction assay, and the volume of the enzyme was always adjusted to produce 6  $\mu$ M/min superoxide.<sup>14</sup> After 20 min, the reaction was stopped by adding 60% acetonitrile to the system.

**2.2. Quantification of Urate Hydroperoxide by Ferrous Oxidation Xylenol Orange (FOX) and Iodometric Assays.** Urate hydroperoxide was quantified by determining the oxidation of ferrous iron in the presence of xylenol orange (FOX assay).<sup>15,16</sup> The method consists of the oxidation of Fe<sup>2+</sup> (ammonium ferrous sulfate salt) to Fe<sup>3+</sup> by hydroperoxide in acid solution. The Fe<sup>3+</sup> complexes with xylenol orange, producing a purple color that absorbs at 540–600 nm.<sup>17</sup> Concentrations of reagents were modified so that 220  $\mu$ L of sample in 10 mM ammonium acetate, pH 6.8, could be added to 80  $\mu$ L of FOX reagent. An aliquot of the reaction system was removed at different time points and incubated with catalase for 5 min; then, the FOX reagent was added, and the samples were left at room temperature for at least 40 min before reading the absorbance at 560 nm using a microplate reader (Synergy H1 hybrid reader). Concentrations were determined from a standard curve for hydrogen

peroxide (H<sub>2</sub>O<sub>2</sub>) and calibrated using  $\epsilon_{240\text{nm}} = 43.6 \text{ M}^{-1} \text{ cm}^{-1}$ .<sup>18</sup> Results are expressed as hydrogen peroxide equivalents.

The quantification of urate hydroperoxide by an iodometric assay was performed as described before.<sup>19</sup> Briefly, 0.5 mL of acetic acid/chloroform (3:2) followed by 0.05 mL of potassium iodide was quickly added to the test tube containing urate hydroperoxide (50  $\mu$ L). Nitrogen gas was introduced in each tube to remove the O<sub>2</sub> content to avoid oxidation other than that coming from urate hydroperoxide. The samples were left to react for 5 min at room temperature in the dark. Then, 1.5 mL of cadmium acetate was added to each tube. The absorbance of these solutions was read in a UV-2550 (Shimadzu) spectrophotometer at 353 nm. The absorbance was plotted against a *tert*-butyl hydroperoxide standard curve to determine the urate hydroperoxide concentration.

**2.3. Characterization of Urate Hydroperoxide by Liquid Chromatography–Electrospray Ionization Tandem Mass Spectrometry.** The products generated by photo-oxidation were analyzed in a Shimadzu HPLC system (Tokyo, Japan) coupled to a Quattro II mass spectrometer (Micromass, Altricham, UK). The products were separated in a TSK-Gel amide-80 (4.6  $\times$  150 mm, 3  $\mu$ m particle size) (Tosoh Bioscience; Tokyo, Japan). The mobile phase was 10 mM ammonium acetate pH 6.8 (solvent A) and acetonitrile (solvent B). The separation was performed in an isocratic mode using 60% solvent B for 20 min with flow rate of 0.2 mL/min. The column was maintained at 25 °C. Immediately before injection, the reaction was diluted (40% reaction and 60% acetonitrile), and 100  $\mu$ L was injected into the HPLC-MS/MS system. Mass spectrometry analyses were done with an electrospray ionization source (ESI) in negative ion mode. The photoproducts were analyzed using full-scan mode (50–400 *m/z*) and product ion scan mode. Urate hydroperoxide and hydroxyisourate were identified by their deprotonated molecules [M – H]<sup>–</sup> at *m/z* 199 and 183, respectively. Source and desolvation temperatures were 100 and 200 °C, respectively. The voltages were 4.5 kV for electrospray, 15 V for sample cone, and 5 V for extractor cone. The collision energy was 10 eV for urate hydroperoxide (*m/z* 199) and 15 eV for hydroxyisourate (*m/z* 183).

For a comparative analysis of the urate hydroperoxide synthesized by photo-oxidation or by enzyme catalysis, its fragmentation pattern was examined in an AmazonSpeed mass spectrometer (Bruker Corporation). Tandem mass fragmentation (MS<sup>3</sup>) was carried out by direct infusion of 5  $\mu$ L of the photo-oxidation or enzyme reaction system (Section 2.1). HPLC separation was performed under the same chromatography conditions as described above. The samples were analyzed in negative ion mode using multiple reaction monitoring (MRM; *m/z* 199  $\rightarrow$  156 and *m/z* 199  $\rightarrow$  112.8 for urate hydroperoxide). The ESI-MS parameters were set as follows: CUR, 20 psi; CAD, medium; IS, 4500 V; temperature, 450 °C; GS1, 55 psi; GS2, 40 psi; and EP, 10 V. The first 5 min of eluent was directed to waste, and the 6–15 min fraction was diverted to the ESI source. The data were processed using Bruker Compass DataAnalysis software.

**2.4. Spectroscopic Analyses of Urate Hydroperoxide.** To determine the molar extinction coefficient of urate hydroperoxide, the compound was synthesized as described in Section 2.1. Briefly, 1.5 mM urate reacted with riboflavin (200  $\mu$ M) in 20 mM phosphate buffer, pH 6.0, under UVA light. After 10 min, 200  $\mu$ L of the reaction was mixed with 300  $\mu$ L of acetonitrile and injected into a 500  $\mu$ L loop. The reaction products were separated by HPLC (Shimadzu, LC-20AT pumps, SPD-20A absorbance detector, and CBM-20A controller connected to LC solution software) in a semipreparative TSK-Gel amide-80 column (10  $\mu$ m; 7.8 mm  $\times$  30 cm). The products were eluted in isocratic mode: 40% 10 mM ammonium acetate pH 6.8 (solvent A) and 60% acetonitrile (solvent B) at a flow rate of 0.8 mL/min for 20 min. Urate hydroperoxide eluted as the major peak; it was collected, and the acetonitrile was dried with nitrogen. The hydroperoxide was diluted in 10 mM ammonium acetate (pH 6.8) to obtain 10, 20, 40, and 100% hydroperoxide. The absorbance of these solutions was read in a UV-2550 (Shimadzu) spectrophotometer (308 nm or scan 230–400 nm) and plotted against the concentration found by the FOX assay (Section 2.2). The extinction coefficient was

obtained by the Lambert–Beer law ( $Abs = \epsilon cl$ ) and is based on hydrogen peroxide equivalents.

**2.5. Kinetics and Identification of the Products from the Spontaneous Decomposition of Urate Hydroperoxide.** To calculate the rate constant for urate hydroperoxide decomposition, the compound was synthesized and isolated as described in Sections 2.1 and 2.4, respectively. The samples were kept at 22 °C in the presence of catalase (20 U/mL), and aliquots were analyzed at different time points for hydroperoxide quantification by FOX assay. Urate hydroperoxide decayed with first-order kinetics; therefore, the calculation was based on a nonlinear fit to the function  $y = y_0 + A^{kx}$ .

The products from urate hydroperoxide decomposition were separated on a TSK-Gel amide-80 column (4.6 × 150 mm, 3 μm particle size) (Tosoh Bioscience; Tokyo, Japan) connected to a HPLC (Shimadzu, LC-20AT pumps). The mobile phase was 10 mM ammonium acetate pH 6.8 (solvent A) and acetonitrile (solvent B). The separation was performed isocratically using 60% solvent B for 20 min at a flow rate of 0.2 mL/min. The absorbance of the products was followed in a diode array detector (SPD M20A, Shimadzu).

**2.6. Reduction Potential of Urate Hydroperoxide.** Electrochemical measurements were performed in a 1 mL, one-compartment cell containing a glassy carbon electrode as the working electrode, a platinum foil auxiliary electrode, and a saturated Ag/AgCl electrode as reference. The surface of the glassy carbon electrode was polished with alumina powder (0.05 μm) on a polishing pad, rinsed with water, and then sonicated with ethanol and water prior to use.<sup>20</sup> A 10 mM ammonium acetate solution was used as the supporting electrolyte, and its pH was corrected to 6.8 by adding an adequate volume of acetic acid. Voltammetric experiments were carried out with a PalmSens potentiostat (Pamsens BV, Houten, Netherlands) controlled using PSTRACE 4.1 software. The pH measurements were performed with a Digimed pH meter. Experiments were carried out at room temperature, 20 ± 1 °C.

**2.7. Evaluation of the Reactivity of Urate Hydroperoxide with Amino Acids.** To determine the susceptibility of amino acids to oxidation by urate hydroperoxide, the compound (40 μM) was incubated with 1 mM histidine, tryptophan, methionine, cysteine, or lysine or 5 mM taurine at 22 °C. Aliquots were removed at different time points for up to 60 min. Catalase (50 U/mL) was added to the aliquots to remove any hydrogen peroxide that could have formed in the samples. The remaining urate hydroperoxide was quantified by the FOX assay. Solutions of 260 μM urate hydroperoxide before and after addition of 300 μM methionine were scanned by UV (230–400 nm) in a Synergy H1 hybrid reader (Biotek, USA) or injected into a semipreparative column (TSK-Gel amide-80 column 10 μm; 7.8 mm × 30 cm). Separation of the product from urate hydroperoxide reduction was performed as described in Section 2.4.

The oxidation products of methionine (300 μM) or cysteine (300 μM) formed by an equimolar concentration of urate hydroperoxide were separated and identified in a Shimadzu HPLC system (Tokyo, Japan) coupled to a Quattro II mass spectrometer (Micromass, Altricham, UK). The products were separated on a TSK-Gel amide-80 (4.6 × 150 mm, 3 μm particle size) (Tosoh Bioscience; Tokyo, Japan). The mobile phase was 10 mM ammonium acetate pH 6.8 (solvent A) and acetonitrile (solvent B). The separation of methionine oxidation products was performed with a linear gradient from 85 to 10% solvent B over 20 min. This was maintained for 10 min and then returned to the initial conditions over 2 min and re-equilibrated for 8 min at a flow rate of 0.8 mL/min. The separation of cysteine oxidation products was performed with a linear gradient from 65 to 10% solvent B over 15 min. This was maintained for 10 min and then returned to the initial conditions over 1 min and equilibrated for 9 min at flow rate of 0.6 mL/min. Mass spectrometry analyses were performed with an electrospray ionization source (ESI) in positive ion mode using full-scan mode (50–300 *m/z*). For methionine oxidation products, source and desolvation temperatures were 150 and 300 °C, respectively. The voltages were 2.5 kV for electrospray, 15 V for sample cone, and 5 V for extractor cone. The collision energy was 10 eV. For cysteine oxidation products, source and desolvation temperatures were 150 and 250 °C, respectively. The voltages were 4 kV for electrospray, 15 V for

sample cone, and 5 V for extractor cone. The collision energy was 10 eV.

**2.8. Assessment of Glutathione (GSH) and Glutathione Disulfide (GSSG) after the Reaction of Glutathione with Urate Hydroperoxide.** Initially, approximately 100 μM urate hydroperoxide was incubated with 500 μM GSH for 10 min at room temperature. The samples were diluted and injected into the HPLC coupled to a CoulArray S600A detector. GSH and GSSG were separated in a Kinetex C18 Phenomenex (2.6 μm; 4.6 mm × 10 cm) column at 25 °C. The mobile phase consisted of 25 mM sodium phosphate buffer, 25 μM octanesulfonic acid, and 1% acetonitrile, pH 2.5 (solvent A), and 1% acetonitrile (solvent B). The separation was carried out at 100% solvent A (0–8 min), which was followed by a gradient from 100 to 0% solvent A (8–9 min), 0% solvent A (9–10 min), and 0 to 100% solvent A (10–11 min), with an equilibrium time of 2 min. GSH and GSSG eluted at 2.5 and 5 min, respectively. GSH was monitored at 400 and 600 mV application potentials, and GSSG, at 950 mV application potential. The peak area was plotted against a standard curve of GSH (0–50 μM) and GSSG (0–30 μM).

**2.9. Kinetics for the Reaction of Urate Hydroperoxide with Glutathione.** Urate hydroperoxide was obtained by photo-oxidation and purified by HPLC (Section 2.1 and 2.4). After quantification ( $\epsilon_{308nm} = 6.54 \pm 0.38 \times 10^3 \text{ M}^{-1} \text{ cm}^{-1}$ ), urate hydroperoxide (7–70 μM) was incubated with glutathione (500 μM) in 10 mM ammonium acetate, pH 7.4. The kinetics was carried out at 23 °C. Aliquots were removed at different time points for hydroperoxide quantification by FOX assay. Urate hydroperoxide and glutathione reacted with first-order kinetics; therefore, the time course of the reaction was analyzed using nonlinear adjustment of the function  $y = y_0 + A^{kx}$ . The initial rate of reaction was determined from this equation and plotted against the initial urate hydroperoxide concentration. The slope of this graph gave the pseudo-first-order rate constant for the reaction of glutathione with urate hydroperoxide. The second-order rate constant was then calculated by dividing the first-order rate constant by the concentration of glutathione (500 μM).

**2.10. Statistical Analyses.** The data are expressed as the mean ± standard error of the mean (SEM). Statistical analyses were performed by one-way analysis of variance (ANOVA) with repeated measures when appropriate (GraphPad Prism 5.0 or OriginPro 8.5). Statistical significance was assessed by *posthoc* comparisons using Bonferroni or Student's *t* test. Results with  $p < 0.05$  were considered to be significant.

### 3. RESULTS

**3.1. Urate Hydroperoxide Synthesis by Photo-oxidation.** The synthesis of urate hydroperoxide was carried out by photo-oxidation using riboflavin as photosensitizer.<sup>11,21</sup> Ten minutes after UVA (365 nm) radiation, 50% of the initial concentration of urate (100–600 μM) was oxidized to urate hydroperoxide. Longer periods of radiation led to the degradation of urate hydroperoxide, as observed by a decrease in the hydroperoxide concentration over time (Figure 1A). Riboflavin absorbs at 221–227, 265–270, and 365–370 nm in the UV and at 445 nm in the visible region.<sup>22</sup> Therefore, we used a visible light source (fluorescent lamps) to compare the production of urate hydroperoxide with visible and UV light sources. Radiation using visible light gave a lower yield of urate hydroperoxide after a 10 min reaction. From this point, we selected UV radiation for use in subsequent experiments (Figure 1B). The addition of superoxide dismutase to the reaction system greatly decreased urate hydroperoxide formation (Figure 1C), confirming that urate hydroperoxide was formed by a superoxide-dependent mechanism.

**3.2. Characterization of Urate Hydroperoxide by Liquid Chromatography–Electrospray Ionization Tandem Mass Spectrometry (HPLC–MS/MS).** To separate and identify the products of urate oxidation, the reaction mixture was injected into a HPLC–MS/MS system. Four peaks with



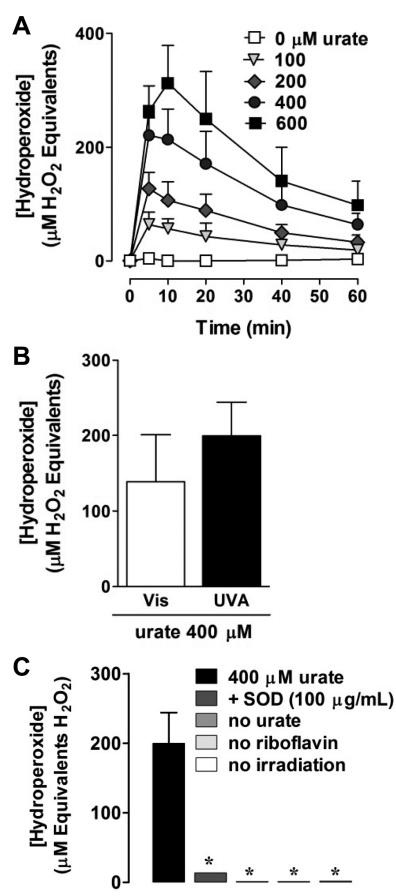


**Figure 1.** Synthesis of urate hydroperoxide by photo-oxidation. (A) Time course of hydroperoxide formation by UVA (365 nm) irradiation in the presence of urate (0–600 μM). (B) Hydroperoxide concentration after 10 min of visible light (Vis) (500 nm) or UVA (365 nm) irradiation in the presence of urate (400 μM). (C) Hydroperoxide concentration after 10 min of UVA (365 nm) irradiation under different conditions. Hydroperoxide was quantified by FOX assay after addition of catalase (10 U/mL) to the samples. Graphs represent mean  $\pm$  SEM of two or three independent experiments. Statistical analyses were performed by one-way ANOVA with repeated measures; \*,  $p < 0.001$  by Bonferroni's posthoc test (B) or Student's  $t$  test (C). SOD, superoxide dismutase.

retention times of 9.3; 10.4; 11.0 and 12.9 min were identified in the UV–vis (302 nm) chromatogram (Figure 2A). The mass scan for each peak revealed ions  $m/z$   $[M - H]^-$  199, 183, 167, and 375, corresponding to urate hydroperoxide, hydroxyisourate, urate, and riboflavin, respectively. The ion corresponding to urate hydroperoxide ( $m/z$   $[M - H]^-$  199) fragmented to the ion products  $m/z$   $[M - H]^-$  156, 139, 111, or 113 and 87. Hydroxyisourate ( $m/z$   $[M - H]^-$  183) was also fragmented and gave  $m/z$   $[M - H]^-$  140, 113, 96, and 69. The fragmentation patterns are represented in Figure 2B,C, and the calculated neutral losses are presented in Table 1.

The characterization of a compound through its fragmentation pattern is a useful tool to accurately identify and quantify molecules. For instance, the identification of an ion product with  $m/z$   $[M - H]^-$  199 that breaks down exactly to the ion products shown in Figure 2B and Table 1 increases the possibility of this product being urate hydroperoxide instead of any other compound with the same  $m/z$ . To obtain an even more precise identification, MS<sup>3</sup> analysis was carried out. To this end, we performed MS<sup>3</sup> and MRM (multiple reaction

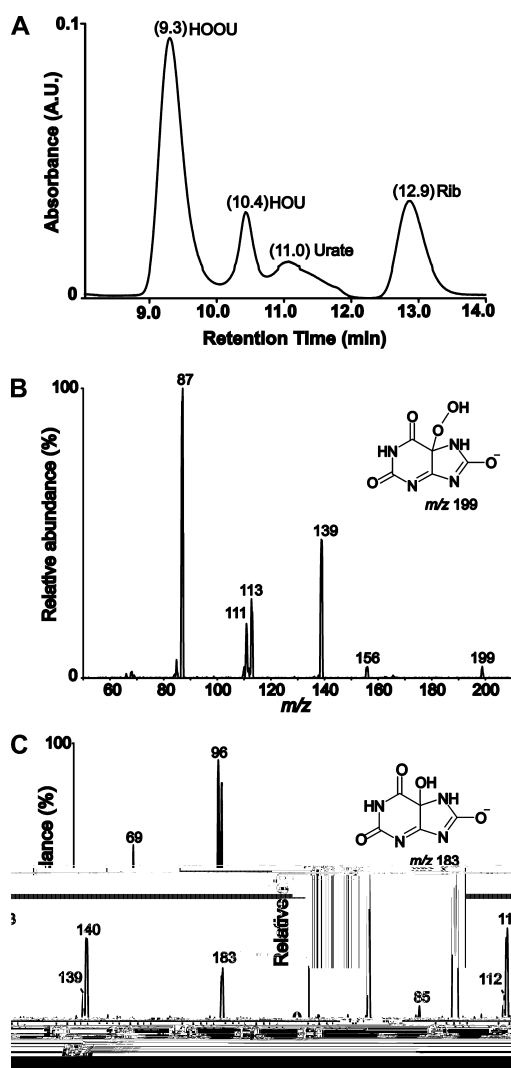


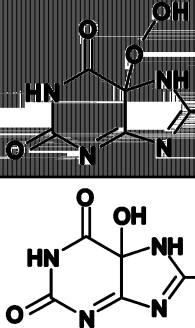
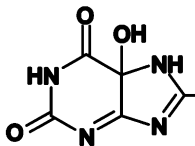
**Figure 2.** Fragmentation pattern of urate hydroperoxide and hydroxyisourate synthesized by photo-oxidation. The separation, identification, and characterization of urate hydroperoxide produced in the reaction of 400 μM urate, 40 μM riboflavin under 10 min UVA irradiation was performed using a triple-quadrupole mass spectrometer (LC-MS/MS). (A) UV–vis chromatogram with detection at 302 nm. (B) MS/MS data from the product eluted at 9.30 min (ion with  $m/z$   $[M - H]^-$  199). (C) MS/MS data from the product eluted at 10.43 min (ion with  $m/z$   $[M - H]^-$  183).

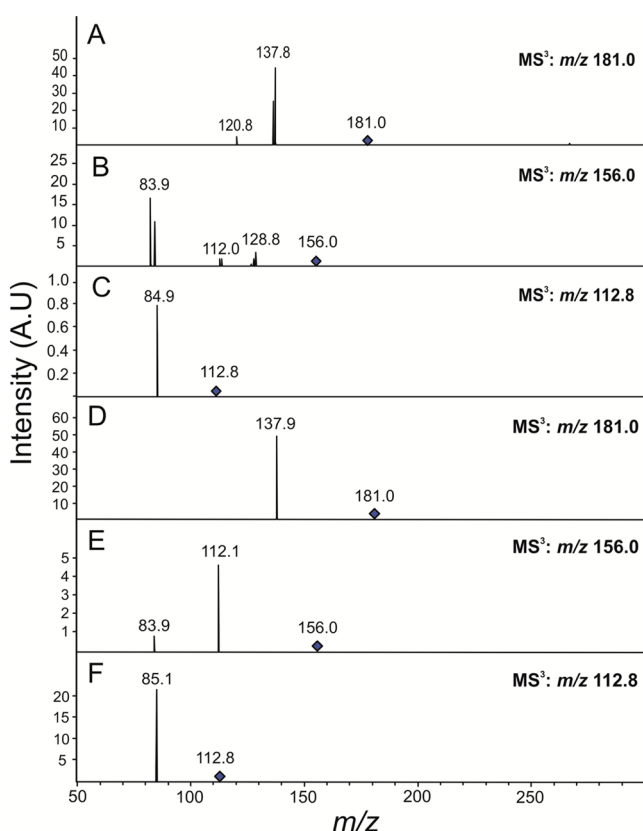
monitoring) using tandem ion trap mass spectrometry. In this experiment, it was possible to compare the products of urate oxidation generated by photo-oxidation and those produced by the reaction with myeloperoxidase and superoxide.

In this experiment, we monitored the ion transitions previously found in the scan mode ( $m/z$   $[M - H]^-$  199  $\rightarrow$  156; 199  $\rightarrow$  112.8; 199  $\rightarrow$  87) (Figure 2B) and the transition  $m/z$   $[M - H]^-$  199  $\rightarrow$  181, which represents a loss of water ( $-H_2O$ ). These ion transitions appeared in both the photo-oxidized and myeloperoxidase-catalyzed reaction systems. Of relevance, fragmentation of the ions  $m/z$   $[M - H]^-$  181, 156, and 112.8 (MS<sup>3</sup>) yielded similar ion products in both systems (Figure 3).

In addition to the MS<sup>3</sup> data, MRM analyses revealed that the ions with mass transitions  $m/z$   $[M - H]^-$  199  $\rightarrow$  156 and 199  $\rightarrow$  112.8, detected in either the photo-oxidized or the myeloperoxidase-catalyzed reaction, had the same retention

**Table 1.** Fragmentation Products of Urate Hydroperoxide and Hydroxyisourate

Compound Structure	Retention Time (min)	Retention Time (min)	Product ions
	9.2	10.4	156 [M-H-CHNO] <sup>-</sup> 160 [M-H-CHN <sub>2</sub> O] <sup>-</sup> 113 [M-H-C <sub>2</sub> H <sub>2</sub> N <sub>2</sub> O] <sup>-</sup> 111 [M-H-C <sub>2</sub> H <sub>2</sub> N <sub>2</sub> O] <sup>-</sup> 87 [M-H-C <sub>2</sub> H <sub>2</sub> N <sub>2</sub> O] <sup>-</sup>
	10.4	183	140 [M-H-CHNO] <sup>-</sup> 113 [M-H-C <sub>2</sub> H <sub>2</sub> N <sub>2</sub> O] <sup>-</sup> 96 [M-H-C <sub>2</sub> H <sub>2</sub> N <sub>2</sub> O] <sup>-</sup> 69 [M-H-C <sub>2</sub> H <sub>2</sub> N <sub>2</sub> O] <sup>-</sup>

**Figure 3.** Tandem mass spectrometry of urate hydroperoxide. Urate hydroperoxide was synthesized by myeloperoxidase in the presence of superoxide and hydrogen peroxide (A–C) or by UV irradiation of urate in the presence of riboflavin and oxygen (D–F). The total reaction (5  $\mu$ L) was directly infused into the mass spectrometer. The peaks represent the spectra of the products ( $MS^3$ ) generated by fragmentation of the ions  $m/z$  181, 156, 112.8; all of them originated from the ion  $m/z$  199.

times. These data confirm that the two species with  $m/z$  199 have the same chemical features regardless of how they were formed (Figure 4). Together, these data support the initial hypothesis that the urate hydroperoxide previously identified in the reaction of urate with myeloperoxidase and superoxide<sup>6</sup> is structurally the same as the urate hydroperoxide generated by photo-oxidation.<sup>11</sup>

### 3.3. Urate Hydroperoxide UV Spectroscopy, Kinetics for Spontaneous Decay, and Decomposition Products.

Because we intended to study the reactivity of urate hydroperoxide with other biological molecules, we first monitored the stability of the compound in water. The stability of urate hydroperoxide is low at room temperature, and it decayed spontaneously in a first-order process. The calculated rate constant was  $k = 2.808 \pm 0.1854 \times 10^{-4} \text{ s}^{-1}$ . By fitting the urate hydroperoxide concentration curve over time, its calculated half-life was determined to be 41 min at 22 °C (Figure 5A). We also followed the decomposition of urate hydroperoxide at 4 °C, which occurred slowly over 10 h. Urate hydroperoxide eluted at 9.2 min (peak 4, Figure 5B). A gradual decrease in absorbance intensity was observed for this peak over time (data not shown). The initial decomposition product was the alcohol, hydroxyisourate (peak 5, Figure 5B). The alcohol also underwent spontaneous decomposition to generate products with maximum absorption at 221 nm (peak 1 and 2, Figure 5B), which is compatible with an open-ring form of hydroxyisourate. The later product (peak 3, Figure 5B) had a maximum absorption at 215 nm and increased gradually over time. This product had the same retention time as that of allantoin (data not shown).

Because urate hydroperoxide decomposed spontaneously, we needed a prompt method to quantify it after purification. For this purpose, we determined the molar extinction coefficient ( $\epsilon$ ) of urate hydroperoxide. The UV scan (220–400 nm) of purified urate hydroperoxide had a maximum absorption at 308 nm (Figure 5C). Plotting urate hydroperoxide absorption at 308 nm against its concentration, determined by the FOX assay (Figure 5D), gave a molar extinction coefficient for urate hydroperoxide of  $\epsilon_{308\text{nm}} = 6.54 \pm 0.38 \times 10^3 \text{ M}^{-1} \text{ cm}^{-1}$ .

Because the stoichiometry for the reaction of peroxides with the FOX reagent varies for different hydroperoxides,<sup>23</sup> we also measured the concentration of urate hydroperoxide by iodometry and compared the concentrations found in both methods. The concentration of hydroperoxide determined by the FOX assay was  $102 \pm 3\%$  ( $n = 2$ ) of that determined by iodometry. This data demonstrates that the response of urate hydroperoxide in the FOX assay is quantitatively the same as that for hydrogen peroxide. Therefore, urate hydroperoxide can be quantified in the FOX assay based on a known concentration of hydrogen peroxide.

### 3.4. Electrochemical Behavior of Urate Hydroperoxide.

Because we were interested in the chemical features and reactivity of urate hydroperoxide, we analyzed its electrochemical behavior by cyclic voltammetry. The experiments were carried out from 1.0 to  $-1.0 \text{ V}$  vs Ag/AgCl. Figure 6A shows the onset of a cathodic process at around  $-0.5 \text{ V}$ , which corresponds to the electrochemical reduction of urate hydroperoxide. We also analyzed the electrochemical behavior of hydroxyisourate, the product of urate hydroperoxide reduction. As expected, no response was noticed at the working potential. Therefore, the product obtained by urate hydroperoxide reduction does not interfere in the cathodic process. In another set of experiments, the voltammograms were recorded at the same potential range but at different concentrations of urate hydroperoxide (Figure 6B). The linearity between urate hydroperoxide concentration and the yielded currents (measured at  $-0.9 \text{ V}$ ) supports the usefulness of this electrochemical method for the rapid detection and quantification of urate hydroperoxide in aqueous solution. The method had low

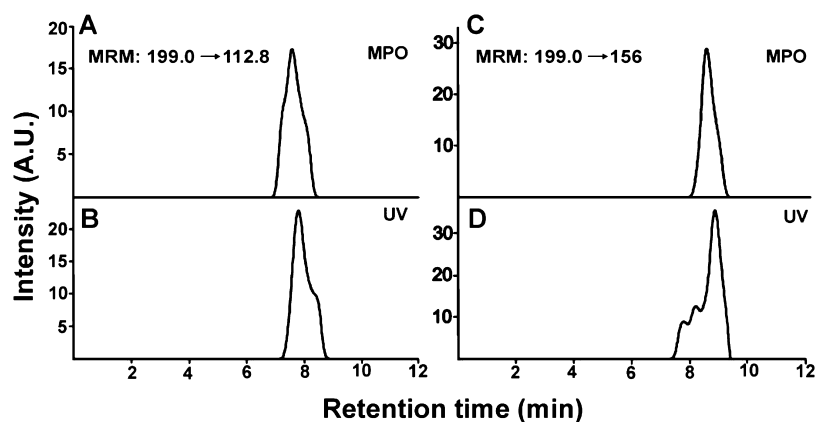


**Figure 4.** Multiple reaction monitoring (MRM) of the oxidation product of urate by photo-oxidation or myeloperoxidase (MPO). Chromatogram peak of the product with mass transitions  $m/z$  199  $\rightarrow$  156 (A) or  $m/z$  199  $\rightarrow$  112.8 (B). The product with a specific mass transition was obtained by reacting urate with myeloperoxidase in the presence of superoxide and hydrogen peroxide (upper panels) or by UV irradiation of urate in the presence of riboflavin and oxygen (lower panels). The reaction mixture (10  $\mu$ L) was injected in a TSK-Gel amide-80 column, and MRM analyses were performed using tandem mass fragmentation. The graphs are representative of three independent experiments.

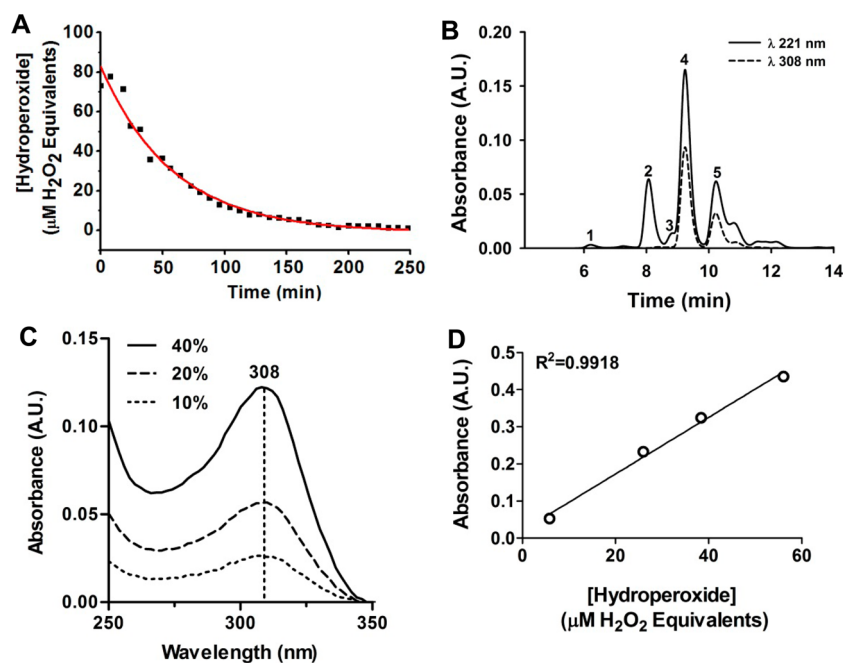


**Figure 5.** Kinetics of decomposition, products formation, and determination of the molar extinction coefficient ( $\epsilon$ ) of urate hydroperoxide. (A) First-order kinetics model adjusted to the observed data of urate hydroperoxide concentration over time (s) at 22 °C. The rate constant was  $k = 2.80 \pm 0.18 \times 10^{-4} \text{ s}^{-1}$ , resulting in a half-life of 41 min. Hydroperoxide was quantified by FOX assay after the addition of catalase (10 U/mL) to the samples. (B) Chromatogram traces of urate hydroperoxide and its spontaneous breakdown products. The urate hydroperoxide solution was injected onto HPLC 3 h after its purification. Traces are representative of the same sample at  $\lambda_{221\text{nm}}$  (solid line) and  $\lambda_{308\text{nm}}$  (dashed line). (C) Urate hydroperoxide absorption spectrum (250–350 nm) obtained after purification of the compound using HPLC and dilution to 40, 20, and 10% in 10 mM ammonium acetate, pH 6.8. The maximum absorption ( $\lambda_{\text{max}}$ ) was achieved at 308 nm. The results are representative of three independent experiments. (D) Linear relationship between absorbance (308 nm) and urate hydroperoxide concentration in ammonium acetate (10 mM, pH 6.8). Hydroperoxide was quantified by a modified FOX assay. Urate hydroperoxide's molar extinction coefficient (308 nm) was  $6.54 \times 10^3 \text{ M}^{-1} \text{ cm}^{-1}$ . Data are representative of three independent experiments.

sensitivity, but it can be enhanced with small modifications in the sensor.

**3.5. Reactivity of Urate Hydroperoxide with Free Amino Acids.** Taking into account the oxidizing potential of urate hydroperoxide, we tested its reactivity with oxidizable amino acids, including taurine, histidine, lysine, tryptophan, methionine, and cysteine.<sup>24</sup> Urate hydroperoxide showed no reactivity toward taurine, lysine, and tryptophan and little with histidine. In contrast, urate hydroperoxide was quickly

consumed by methionine or cysteine (Figure 7A). When it reacted with methionine, there was a shift in the UV maximal absorption ( $\lambda_{\text{max}}$  308  $\rightarrow$  304 nm) (Figure 7B), and, as judged by HPLC (Figure 7C), it was reduced to its corresponding alcohol.<sup>12,25</sup>

The oxidation products of methionine were identified by LC-MS/MS. The oxidation product eluted at 12 min, and the remaining nonoxidized methionine eluted at 9.8 min (Figure 7D, upper panel). The product that eluted at 12 min had an  $m/$

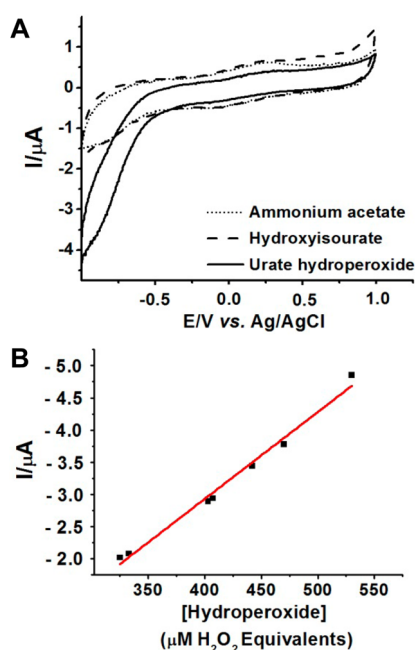


**Figure 6.** Analyses of the redox potential of urate hydroperoxide. (A) Voltammograms were recorded at  $100 \text{ mV s}^{-1}$  with a glassy carbon electrode. Urate hydroperoxide and its corresponding alcohol, hydroxyisourate, were synthesized by photo-oxidation and purified by HPLC. They were diluted to  $500 \text{ } \mu\text{M}$  in  $10 \text{ mM}$  ammonium acetate,  $\text{pH } 6.8$ . This is only an estimated concentration for hydroxyisourate. The solid line (—) represents urate hydroperoxide, dashed line (---) represents hydroxyisourate, and dotted line (.....) represents ammonium acetate. (B) Relationship between the current measured at  $-0.9 \text{ V}$  and urate hydroperoxide concentration. Urate hydroperoxide concentration was obtained by its molar extinction coefficient  $\epsilon_{308\text{nm}} = 6.54 \times 10^3 \text{ M}^{-1} \text{ s}^{-1}$ . The graphs are representative of three independent experiments.

$z [\text{M} - \text{H}]^+$  of  $166 \text{ Da}$ , which corresponds to the expected increase in mass of  $16 \text{ Da}$  for methionine sulfoxide due to incorporation of oxygen into the molecule. The MS/MS spectra of this product is represented at Figure 7D (lower panel). The neutral loss generated the ion fragments  $m/z [\text{M} - \text{H}]^+$   $149$ ,  $102$ , and  $74$ . This is presented in the Table 2, and the data are consistent with those expected for methionine sulfoxide.<sup>26–28</sup>

The incubation of an equimolar concentration of cysteine and urate hydroperoxide completely consumed cysteine to generate an oxidized product that eluted at  $11.6 \text{ min}$  (Figure 7E, upper panel). The oxidation product had an  $m/z [\text{M} - \text{H}]^+$  of  $241 \text{ Da}$ , which corresponds to cystine. The MS/MS spectra of this product gave a series of fragments (Figure 7E, lower panel), and the neutral losses for these ion fragments are presented in Table 2 and are consistent with those expected for cystine.<sup>29–31</sup>

**3.6. Kinetics and Mechanisms of Oxidation of Glutathione by Urate Hydroperoxide.** We previously reported that urate hydroperoxide reacts with glutathione.<sup>6</sup> Here, we calculated the rate constant for this reaction. Urate hydroperoxide was reacted with glutathione under pseudo-first-order conditions and showed a single-exponential decay (Figure 8A). Using linear regression, we calculated a second-order rate constant of  $13.7 \pm 0.8 \text{ M}^{-1} \text{ s}^{-1}$  for the reaction between urate hydroperoxide and glutathione at  $23 \text{ }^\circ\text{C}$ ,  $\text{pH } 7.4$  (Figure 8B).

Next, we investigated the mechanisms of the reaction between glutathione and urate hydroperoxide and looked for the formation of a possible adduct as a specific marker for urate hydroperoxide oxidation. After incubation with urate hydroperoxide, all consumed GSH ( $120 \text{ } \mu\text{M}$ ) was converted to GSSG ( $57 \text{ } \mu\text{M}$ ), representing  $2:1$  stoichiometry. Therefore, there was no detectable adduct formed between glutathione–urate hydroperoxide (Figure 8C).

#### 4. DISCUSSION

Urate has been considered to be a key antioxidant in human plasma,<sup>1,32,33</sup> but its role as an antioxidant has been contradicted by the positive correlation between high levels of urate and the progression of oxidative stress related diseases.<sup>34–38</sup> The dual effect of urate is clearly dependent on the environment and on the oxidizing/reducing species involved.<sup>32,39</sup> In the absence of other reactants, the urate free radical produced by peroxidase/ $\text{H}_2\text{O}_2$  can dismutate to yield dehydrourate, which hydrolyzes to the inert product, allantoin. However, in the presence of superoxide radical, as occurs in the oxidative inflammatory burst of neutrophils, both radicals can combine to form urate hydroperoxide.<sup>6</sup> Urate hydroperoxide is more stable than its free radical precursor and may oxidize biomolecules. Thus, the formation of this intermediate would explain the pro-oxidant effect of urate and its ability to inactivate enzymes sensitive to oxidative stress.<sup>40,41</sup> As previously reported, the release of the monocyte chemotactic protein-1 induced by uric acid occurs only in the presence of superoxide.<sup>42</sup> Therefore, the chemical identification and characterization of urate hydroperoxide will contribute to the comprehension of the pro-oxidant mechanisms of urate during oxidative stress and inflammatory disorders.

The formation of an organic peroxide as an intermediate in urate oxidation by mammalian peroxidases and by exposing milk to irradiation was previously identified,<sup>6,9,11</sup> but no additional chemical information on this peroxide was provided. To chemically characterize this peroxide, it was necessary to have enough of the product to perform a mass spectrometry scan and to identify the fragmentation pattern of the molecule. Therefore, the chemical synthesis of the peroxide by photo-oxidation was a good alternative to enzymatic production; thus, we improved the method previously established.<sup>11</sup> Under our conditions, the best methodology for producing urate hydroperoxide was a short exposure of urate, riboflavin, and oxygen to UV light. Under the conditions of the synthesis, riboflavin absorbs light and generates a metastable triplet excited state ( $^3\text{Rib}^*$ ). The return of  $^3\text{Rib}^*$  to the ground state may occur by energy transfer to triplet ground-state oxygen to form singlet oxygen ( $^1\text{O}_2$ ), which is Type II photo-oxidation. Alternatively, triplet riboflavin may abstract hydrogen or electrons from another substrate, yielding free radical intermediates, via a Type I photo-oxidation mechanism.<sup>43,44</sup> In Type I photo-oxidation, riboflavin would catalyze the electron transfer from urate to oxygen to generate urate free radical and superoxide (graphical abstract). In our experiments, peroxide synthesis was mainly due to Type I photo-oxidation because scavenging the superoxide anion radical with superoxide dismutase greatly inhibited hydroperoxide production.

Type II photo-oxidation is also possible in this system because urate is an effective scavenger of singlet oxygen,<sup>1</sup> but the reaction of urate with singlet oxygen is expected to generate unstable dioxetane<sup>45,46</sup> rather than urate hydroperoxide. In agreement with this, the exposure of urate to visible light in the



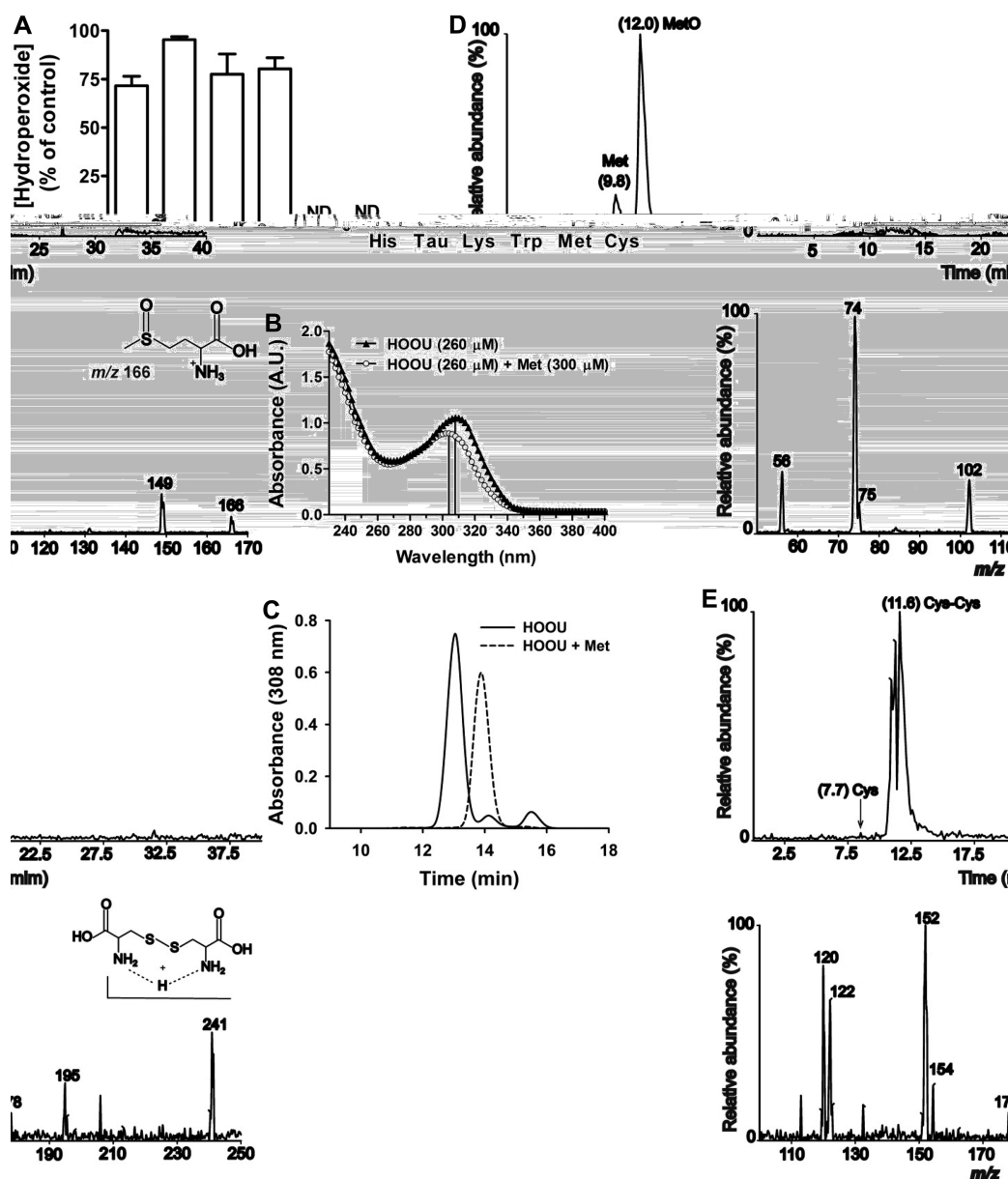


**Figure 7.** Reactivity of urate hydroperoxide with free amino acids. (A) Percentage of urate hydroperoxide concentration after 10 min of incubation (22 °C) with histidine, lysine, tryptophan, methionine, or cysteine (1 mM) or taurine (5 mM) in the presence of catalase (50 U/mL). Hydroperoxide was quantified by FOX assay. Data are mean  $\pm$  SEM of three independent experiments. ND, not detectable. (B) Absorption spectrum (220–400 nm) of urate hydroperoxide (260  $\mu$ M) before and after reaction (1 s) with methionine (300  $\mu$ M). The maximum absorption ( $\lambda_{\max}$ ) was 308 and 304 nm, respectively. (C) Chromatogram of urate hydroperoxide (HOOU) and urate hydroperoxide incubated with methionine (500  $\mu$ M); A.U., arbitrary units. Total ion chromatogram (TIC) and fragmentation pattern of the oxidation products of methionine (D) and cysteine (E) generated by incubation with an equimolar concentration of urate hydroperoxide (300  $\mu$ M).

presence of methylene blue, a singlet oxygen generator, produced a barely detectable amount of hydroperoxide (data not shown).

The fragmentation pattern found for urate hydroperoxide suggested that it was predominately the regioisomer, 5-hydroperoxide (structure represented in the graphical abstract). In accordance with this, thermodynamic studies performed with a similar derivative, 5-hydroperoxy-8-oxo-7,8-dihydroguanosine, demonstrated that this regioisomer is much more stable than 4-hydroperoxy-8-oxo-7,8-dihydroguanosine.<sup>47</sup> Using tandem ion trap mass spectrometry, we identified that the urate hydroperoxide formed by photo-oxidation or enzymatically with MPO, hydrogen peroxide, and superoxide (MPO/H<sub>2</sub>O<sub>2</sub>/O<sub>2</sub><sup>•-</sup>)

is structurally the same. Therefore, the photo-oxidation of urate became a useful tool to obtain higher quantities of pure urate hydroperoxide that will help in the study of the biological effects of this pro-oxidant.

The spectroscopic characterization of urate hydroperoxide and the determination of its molar extinction coefficient are useful for rapidly quantifying the compound. Of relevance, the molar extinction coefficient found in our experiment was similar to that previously proposed for urate hydroperoxide formed by urate oxidase.<sup>12</sup> It is important to mention that the molar extinction coefficient for urate hydroperoxide was calculated relative to a hydrogen peroxide standard curve in the FOX assay. Because the stoichiometry of the FOX reaction

**Table 2.** Fragmentation Products of Methionine Sulfoxide and Cystine

Compound Structure	Retention time (min)	[M+H] <sup>+</sup> (m/z)	Product ions (m/z)
	12	166	149 [M+H- NH <sub>3</sub> ] <sup>+</sup> 102 [M+H- CH <sub>3</sub> SO] <sup>+</sup> 74 [M+H- C <sub>3</sub> H <sub>8</sub> SO] <sup>+</sup>
	11.6	241	195 [M+H- H <sub>2</sub> O+CO] <sup>+</sup> 178 [M+H- H <sub>2</sub> O+CO+NH <sub>3</sub> ] <sup>+</sup> 154 [M+H- C <sub>3</sub> H <sub>5</sub> NO <sub>2</sub> ] <sup>+</sup> 152 [M+H- C <sub>3</sub> H <sub>5</sub> NO <sub>2</sub> +2H] <sup>+</sup> 122 [M+H- C <sub>3</sub> H <sub>5</sub> NSO <sub>2</sub> ] <sup>+</sup>

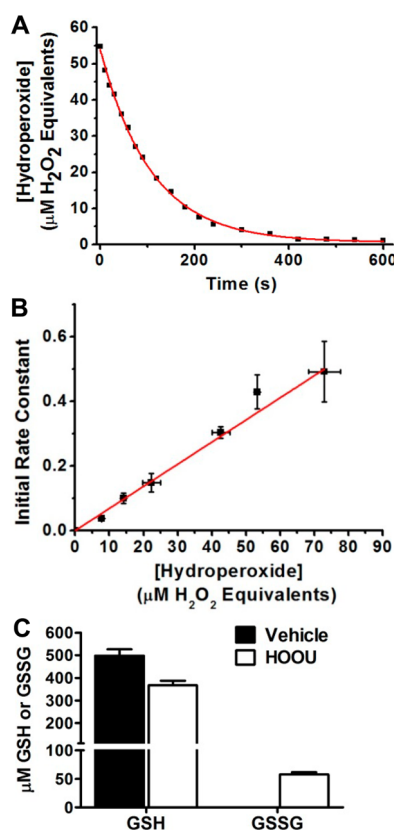


**Figure 8.** Kinetics and mechanism for the oxidation of GSH by urate hydroperoxide (A) Single-order exponential decay of urate hydroperoxide (50  $\mu\text{M}$ ) in the presence of GSH (500  $\mu\text{M}$ ) in 10 mM ammonium acetate, pH 7.4, at 23  $^{\circ}\text{C}$ . The remaining concentration of urate hydroperoxide was measured at time 0 (no GSH) and different time points after GSH addition by FOX assay. (B) Linear regression of the urate hydroperoxide concentration versus the initial rate constant ( $k_{\text{obs}}$  multiplied by the initial concentration of urate hydroperoxide). (C) GSH (500  $\mu\text{M}$ ) was incubated with urate hydroperoxide (100  $\mu\text{M}$ ) or vehicle (10 mM ammonium acetate, pH 6.8) for 10 min at room temperature. GSH and GSSG analyses were performed by HPLC with electrochemical detection using a standard curve for quantification. Graph represents mean  $\pm$  SEM of five independent experiments.

is different for hydrogen peroxide (2.2  $\text{Fe}^{3+}/1 \text{H}_2\text{O}_2$ ) and organic peroxides (4.9  $\text{Fe}^{3+}/1 \text{ROOH}$ ),<sup>23</sup> we validated our data by comparing the concentration of urate hydroperoxide detected in FOX and iodometric assays. The concentration of urate hydroperoxide found in these assays was very similar.

Hence, it was possible to calculate the molar extinction coefficient by iodometric assay,  $\epsilon_{308\text{nm}} = 6.82 \times 10^3 \text{ M}^{-1} \text{ s}^{-1}$ .

Urate hydroperoxide was reduced when it was subjected to an electrical potential, which confirmed that is indeed an oxidizing agent. Taking into account its oxidizing property, we tested urate hydroperoxide's reactivity with taurine, histidine, lysine, tryptophan, methionine, and cysteine, amino acids that are susceptible to oxidation.<sup>24</sup> The oxidative modification of amino acid side chains can alter a protein's structure and function. Urate hydroperoxide reacted specifically with methionine and cysteine. This result shows the selectivity of urate hydroperoxide for sulfur-containing biomolecules. We also tested the reactivity of urate hydroperoxide with taurine, which is not a component of protein but is an abundant free amino acid in the cytosol of immune cells<sup>48</sup> and that could act as a scavenger of urate hydroperoxide.

The oxidation of methionine by urate hydroperoxide occurred by a classical two-electron redox mechanism, forming hydroxyisourate. Hydroxyisourate is an unstable compound itself. It decays with a rate constant of  $2.1 \times 10^{-3} \text{ s}^{-1}$ . A break in the carbon–nitrogen link in the six-member ring has been proposed for the decomposition of hydroxyisourate.<sup>12</sup> A spiroiminodihydantoin intermediate was found in the breakdown of a similar compound, 5-hydroxy-8-oxo-7,8-dihydroguanosine.<sup>49,50</sup>

In our hands, the spontaneous decomposition of urate hydroperoxide and hydroxyisourate gave two isomers with maximal absorption at 221 nm, which is similar to that found by Kahn and Tipton.<sup>12</sup> The formation of isomers in the breakdown of hydroxyisourate was identified before.<sup>51</sup> With longer periods, we observed the peak of a product with maximal absorption at 215 nm that eluted at the same retention time as that of allantoin. Therefore, allantoin is likely to be the major final product of spontaneous urate hydroperoxide decomposition.

Corroborating the evidence for a two-electron oxidation of methionine by urate hydroperoxide, the main detectable product of this reaction was methionine sulfoxide ( $m/z$  [M – H]<sup>+</sup> 166). The fragmentation of methionine sulfoxide generated ions  $m/z$  [M – H]<sup>+</sup> 149, 102, and 74, corresponding to the loss of ammonia, a break in the carbon–sulfur link from the lateral chain, and a rupture in the lateral chain, respectively.<sup>26–28</sup> (Table 2). The oxidation of cysteine generated a product with  $m/z$  [M – H]<sup>+</sup> 241, which is the expected mass for the cysteine disulfide bond dimer, cystine. This was confirmed by the ion fragments from  $m/z$  [M – H]<sup>+</sup> 241 (Table 2), which have also been demonstrated elsewhere.<sup>29–31</sup> From this data, we conclude that the oxidation of cysteine by urate hydroperoxide does not produce a stable adduct.

Urate hydroperoxide reacts with glutathione,<sup>6</sup> and the rate constant for this reaction is nearly 16 times faster than the oxidation of glutathione by hydrogen peroxide<sup>52</sup> and four times faster than the reaction between cysteine and hydrogen peroxide,<sup>52,53</sup> proving that urate hydroperoxide is a more reactive oxidant than hydrogen peroxide. Taking into consideration the enormous amount of proteins with free thiols in the biological milieu, it is expected that urate hydroperoxide would react with these thiol proteins rather than with glutathione. The oxidation of glutathione by urate hydroperoxide also occurred by a two-electron mechanism, and no detectable adducts were found.

In summary, we have presented the chemical characterization of an important intermediate in urate oxidation, urate hydroperoxide, a pro-oxidant compound that can be generated under conditions of inflammation and photo-oxidation. This study supports the need for further investigation of urate hydroperoxide in physiological and pathological processes that are related to inflammation and hyperuricemia as a way to clarify the paradox surrounding the pro- and antioxidant actions of urate.

## AUTHOR INFORMATION

### Corresponding Author

\*Phone: (+55) 11 3091-9069. E-mail: [flaviam@iq.usp.br](mailto:flaviam@iq.usp.br) or [fcmeotti@gmail.com](mailto:fcmeotti@gmail.com).

### Funding

Fundação de Amparo à Pesquisa do Estado de São Paulo (FAPESP), Project Grants 2011/18106-4 and 2013/07937-8 (CEPID-REDOXOMA); Conselho Nacional de Desenvolvimento Científico e Tecnológico (CNPq) Project 472105/2012-4, Núcleo de Apoio à Pesquisa da Universidade de São Paulo (NAP-REDOXOMA). Eliziane Patrício and Larissa da Costa Carvalho received scholarships from FAPESP (2011/15297-3 and 2013/02195-3). Railmara Pereira da Silva and Marcus Camargo Prates received scholarships from CNPq.

### Notes

The authors declare no competing financial interest.

## ACKNOWLEDGMENTS

We thank Dr. Filipe Lima (IQ-USP) for the support on kinetics studies, Adriano de Britto Chaves Filho for iodometric assay support, Professor Maurício Baptista for use of UV device, Professor Marisa Medeiros for the equipment devices ion trap mass spectrometer and HPLC-CoulArray 5600A detector, Professor Antônio Eduardo Miller Crotti (FFCLRP-USP) and Professor Giuseppe Palmisano (ICB-USP) for the support on mass spectrometry and fragmentation pattern discussion.

## ABBREVIATIONS

AU, arbitrary units; ESI, electrospray ionization source; FOX, ferrous oxidation xylene; GSH, glutathione; GSSG, glutathione disulfide; HOOu, urate hydroperoxide; HOU, hydroxyisourate; ISC, intersystem conversion; MRM, multiple reaction monitoring; Rib, riboflavin; ROOH, organic hydroperoxide; SOD, superoxide dismutase; TIC, total ion chromatogram; UVA, ultraviolet A; Vis, visible

## REFERENCES

- (1) Ames, B. N., Cathcart, R., Schwiers, E., and Hochstein, P. (1981) Uric acid provides an antioxidant defense in humans against oxidant- and radical-caused aging and cancer: a hypothesis. *Proc. Natl. Acad. Sci. U. S. A.* 78, 6858–6862.
- (2) Grootveld, M., Halliwell, B., and Moorhouse, C. P. (1987) Action of uric acid, allopurinol and oxypurinol on the myeloperoxidase-derived oxidant hypochlorous acid. *Free Radical Res.* 4, 69–76.
- (3) Winterbourn, C. C. (1985) Comparative reactivities of various biological compounds with myeloperoxidase-hydrogen peroxide-chloride, and similarity of the oxidant to hypochlorite. *Biochim. Biophys. Acta, Gen. Subj.* 840, 204–210.
- (4) Kaur, H., and Halliwell, B. (1990) Action of Biologically-Relevant Oxidizing Species Upon Uric-Acid - Identification of Uric-Acid Oxidation-Products. *Chem.-Biol. Interact.* 73, 235–247.
- (5) Canellakis, E. S., Tuttle, A. L., and Cohen, P. P. (1955) A comparative study of the end-products of uric acid oxidation by peroxidases. *J. Biol. Chem.* 213, 397–404.
- (6) Meotti, F. C., Jameson, G. N., Turner, R., Harwood, D. T., Stockwell, S., Rees, M. D., Thomas, S. R., and Kettle, A. J. (2011) Urate as a physiological substrate for myeloperoxidase: implications for hyperuricemia and inflammation. *J. Biol. Chem.* 286, 12901–12911.
- (7) Maples, K. R., and Mason, R. P. (1988) Free-Radical Metabolite of Uric-Acid. *J. Biol. Chem.* 263, 1709–1712.
- (8) Padiglia, A., Medda, R., Longu, S., Pedersen, J. Z., and Floris, G. (2002) Uric acid is a main electron donor to peroxidases in human blood plasma. *Med. Sci. Monit.* 8, BR454–459.
- (9) Seidel, A., Parker, H., Turner, R., Dickerhof, N., Khalilova, I. S., Wilbanks, S. M., Kettle, A. J., and Jameson, G. N. (2014) Uric acid and thiocyanate as competing substrates of lactoperoxidase. *J. Biol. Chem.* 289, 21937–21949.
- (10) Santos, R., Patterson, L. K., Filipe, P., Morliere, P., Hug, G. L., Fernandes, A., and Maziere, J. C. (2001) Redox reactions of the urate radical/urate couple with the superoxide radical anion, the tryptophan neutral radical and selected flavonoids in neutral aqueous solutions. *Free Radical Res.* 35, 129–136.
- (11) Clausen, M. R., Huvaere, K., Skibsted, L. H., and Staged, J. (2010) Characterization of peroxides formed by riboflavin and light exposure of milk. Detection of urate hydroperoxide as a novel oxidation product. *J. Agric. Food Chem.* 58, 481–487.
- (12) Kahn, K., and Tipton, P. A. (1998) Spectroscopic characterization of intermediates in the urate oxidase reaction. *Biochemistry* 37, 11651–11659.
- (13) Sarma, A. D., and Tipton, P. A. (2000) Evidence for urate hydroperoxide as an intermediate in the urate oxidase reaction. *J. Am. Chem. Soc.* 122, 11252–11253.
- (14) Fridovich, I. (1985) *Handbook of Methods for Oxygen Radical Research*, CRC Press Inc., Boca Raton, FL.
- (15) Winterbourn, C. C., Parsons-Mair, H. N., Gebicki, S., Gebicki, J. M., and Davies, M. J. (2004) Requirements for superoxide-dependent tyrosine hydroperoxide formation in peptides. *Biochem. J.* 381, 241–248.
- (16) Wolff, S. P. (1994) Ferrous ion oxidation in presence of ferric ion indicator xylenol orange for measurement of hydroperoxides. *Methods Enzymol.* 233, 182–189.
- (17) Nourooz-Zadeh, J. (1999) Ferrous ion oxidation in presence of xylenol orange for detection of lipid hydroperoxides in plasma. *Methods Enzymol.* 300, 58–62.
- (18) Beers, R. F., Jr., and Sizer, I. W. (1952) A spectrophotometric method for measuring the breakdown of hydrogen peroxide by catalase. *J. Biol. Chem.* 195, 133–140.
- (19) Buege, J. A., and Aust, S. D. (1978) Microsomal lipid peroxidation. *Methods Enzymol.* 52, 302–310.
- (20) Cancino, J., and Machado, S. A. S. (2012) Microelectrode array in mixed alkanethiol self-assembled monolayers: Electrochemical studies. *Electrochim. Acta* 72, 108–113.
- (21) Cardoso, D. R., Homem-de-Mello, P., Olsen, K., da Silva, A. B., Franco, D. W., and Skibsted, L. H. (2005) Deactivation of triplet-excited riboflavin by purine derivatives: important role of uric acid in light-induced oxidation of milk sensitized by riboflavin. *J. Agric. Food Chem.* 53, 3679–3684.
- (22) Kurtin, W. E., and Song, P. S. (1968) Photochemistry of the model phototropic system involving flavins and indoles. I. Fluorescence polarization and MO calculations of the direction of the electronic transition moments in flavins. *Photochem. Photobiol.* 7, 263–273.
- (23) Gay, C., Collins, J., and Gebicki, J. M. (1999) Determination of hydroperoxides by the ferric-xylenol orange method. *Redox Rep.* 4, 327–328.
- (24) Stadtman, E. R., and Levine, R. L. (2003) Free radical-mediated oxidation of free amino acids and amino acid residues in proteins. *Amino Acids* 25, 207–218.



- (25) Wrona, M. Z., and Dryhurst, G. (1979) Investigation of the Enzymic and Electrochemical Oxidation of Uric-Acid Derivatives. *Biochim. Biophys. Acta* 570, 371–387.
- (26) Peskin, A. V., Turner, R., Maghzal, G. J., Winterbourn, C. C., and Kettle, A. J. (2009) Oxidation of methionine to dehydromethionine by reactive halogen species generated by neutrophils. *Biochemistry* 48, 10175–10182.
- (27) O'Hair, R. A. J., and Reid, G. E. (1999) Neighboring group versus cis-elimination mechanisms for side chain loss from protonated methionine, methionine sulfoxide and their peptides. *Eur. Mass Spectrom.* 5, 325–334.
- (28) Ignasiak, M., Scuderi, D., de Oliveira, P., Pedzinski, T., Rayah, Y., and Levin, C. H. (2011) Characterization by mass spectrometry and IRMPD spectroscopy of the sulfoxide group in oxidized methionine and related compounds. *Chem. Phys. Lett.* 502, 29–36.
- (29) Steill, J. D., Szczepanski, J., Oomens, J., Eyler, J. R., and Brajter-Toth, A. (2011) Structural characterization by infrared multiple photon dissociation spectroscopy of protonated gas-phase ions obtained by electrospray ionization of cysteine and dopamine. *Anal. Bioanal. Chem.* 399, 2463–2473.
- (30) Lioe, H., and O'Hair, R. A. (2007) Comparison of collision-induced dissociation and electron-induced dissociation of singly protonated aromatic amino acids, cystine and related simple peptides using a hybrid linear ion trap-FT-ICR mass spectrometer. *Anal. Bioanal. Chem.* 389, 1429–1437.
- (31) Lioe, H., and O'Hair, R. A. (2007) A novel salt bridge mechanism highlights the need for nonmobile proton conditions to promote disulfide bond cleavage in protonated peptides under low-energy collisional activation. *J. Am. Soc. Mass Spectrom.* 18, 1109–1123.
- (32) Domazou, A. S., Zhu, H., and Koppenol, W. H. (2012) Fast repair of protein radicals by urate. *Free Radical Biol. Med.* 52, 1929–1936.
- (33) Becker, B. F. (1993) Towards the physiological function of uric acid. *Free Radical Biol. Med.* 14, 615–631.
- (34) Alderman, M. H. (2007) Podagra, uric acid, and cardiovascular disease. *Circulation* 116, 880–883.
- (35) Benzie, I. F., and Strain, J. J. (1996) The ferric reducing ability of plasma (FRAP) as a measure of "antioxidant power": the FRAP assay. *Anal. Biochem.* 239, 70–76.
- (36) Nakagawa, T., Kang, D. H., Feig, D., Sanchez-Lozada, L. G., Srinivas, T. R., Sautin, Y., Ejaz, A. A., Segal, M., and Johnson, R. J. (2006) Unearthing uric acid: an ancient factor with recently found significance in renal and cardiovascular disease. *Kidney Int.* 69, 1722–1725.
- (37) Viazzi, F., Parodi, D., Leoncini, G., Parodi, A., Falqui, V., Ratto, E., Vettoretti, S., Bezante, G. P., Del Sette, M., Deferrari, G., and Pontremoli, R. (2005) Serum uric acid and target organ damage in primary hypertension. *Hypertension* 45, 991–996.
- (38) So, A., and Thorens, B. (2010) Uric acid transport and disease. *J. Clin. Invest.* 120, 1791–1799.
- (39) Santos, C. X., Anjos, E. I., and Augusto, O. (1999) Uric acid oxidation by peroxynitrite: multiple reactions, free radical formation, and amplification of lipid oxidation. *Arch. Biochem. Biophys.* 372, 285–294.
- (40) Aruoma, O. I., and Halliwell, B. (1989) Inactivation of alpha 1-antitrypsinase by hydroxyl radicals. The effect of uric acid. *FEBS Lett.* 244, 76–80.
- (41) Kittridge, K. J., and Willson, R. L. (1984) Uric-Acid Substantially Enhances the Free Radical-Induced Inactivation of Alcohol-Dehydrogenase. *FEBS Lett.* 170, 162–164.
- (42) Baldwin, W., McRae, S., Marek, G., Wymer, D., Pannu, V., Baylis, C., Johnson, R. J., and Sautin, Y. Y. (2011) Hyperuricemia as a mediator of the proinflammatory endocrine imbalance in the adipose tissue in a murine model of the metabolic syndrome. *Diabetes* 60, 1258–1269.
- (43) Lu, C. Y., and Liu, Y. Y. (2002) Electron transfer oxidation of tryptophan and tyrosine by triplet states and oxidized radicals of flavin sensitizers: a laser flash photolysis study. *Biochim. Biophys. Acta, Gen. Subj.* 1571, 71–76.
- (44) Sharman, W. M., Allen, C. M., and van Lier, J. E. (2000) Role of activated oxygen species in photodynamic therapy. *Methods Enzymol.* 319, 376–400.
- (45) Foote, C. S. (1995) *Active O<sub>2</sub> in Chemistry*, 4th ed., Blackie, London.
- (46) Halliwell, B., and Gutteridge, J. M. (2007) *Free Radicals in Biology and Medicine*, 4th ed., Oxford University Press Inc., New York.
- (47) McCallum, J. E., Kuniyoshi, C. Y., and Foote, C. S. (2004) Characterization of 5-hydroxy-8-oxo-7,8-dihydroguanosine in the photosensitized oxidation of 8-oxo-7,8-dihydroguanosine and its rearrangement to spiroiminodihydantoin. *J. Am. Chem. Soc.* 126, 16777–16782.
- (48) Learn, D. B., Fried, V. A., and Thomas, E. L. (1990) Taurine and Hypotaurine Content of Human-Leukocytes. *J. Leukoc. Biol.* 48, 174–182.
- (49) McCallum, J. E., Kuniyoshi, C. Y., and Foote, C. S. (2004) Characterization of 5-hydroxy-8-oxo-7,8-dihydroguanosine in the photosensitized oxidation of 8-oxo-7,8-dihydroguanosine and its rearrangement to spiroiminodihydantoin. *J. Am. Chem. Soc.* 126, 16777–16782.
- (50) Martinez, G. R., Medeiros, M. H., Ravanat, J. L., Cadet, J., and Di Mascio, P. (2002) [<sup>18</sup>O]-labeled singlet oxygen as a tool for mechanistic studies of 8-oxo-7,8-dihydroguanine oxidative damage: detection of spiroiminodihydantoin, imidazolone and oxazolone derivatives. *Biol. Chem.* 383, 607–617.
- (51) Kahn, K., Serfozo, P., and Tipton, P. A. (1997) Identification of the true product of the urate oxidase reaction. *J. Am. Chem. Soc.* 119, 5435–5442.
- (52) Winterbourn, C. C., and Metodiewa, D. (1999) Reactivity of biologically important thiol compounds with superoxide and hydrogen peroxide. *Free Radical Biol. Med.* 27, 322–328.
- (53) Radi, R., Beckman, J. S., Bush, K. M., and Freeman, B. A. (1991) Peroxynitrite oxidation of sulfhydryls. The cytotoxic potential of superoxide and nitric oxide. *J. Biol. Chem.* 266, 4244–4250.